GEOPHYSICAL RESEARCH LETTERS, VOL. 27, NO. 3, PAGES 437-440, FEBRUARY 1, 2000

GPS geodetic constraints on Caribbean-North America plate motion

Charles DeMets[1], Pamela E. Jansma[2], Glen S. Mattioli[2], Timothy H. Dixon[3], Fred Farina[3], Roger Bilham[4], Eric Calais[5], and Paul Mann[6]

Abstract. We describe a model for Caribbean plate motion based on GPS velocities of four sites in the plate interior and two azimuths of the Swan Islands transform fault. The data are well fit by a single angular velocity, with average misfits approximately equal to the 1.5-3.0 mm yr^{-1} velocity uncertainties. The new model predicts Caribbean-North America motion ~65% faster than predicted by NUVEL-1A, averaging 18-20±3 mm yr^{-1} (2σ) at various locations along the plate boundary. The data are best fit by a rotation pole that predicts obliquely convergent motion along the plate boundary east of Cuba, but are fit poorly by a suite of previously published models that predict strike-slip motion in this region. The data suggest an approximate upper bound of 4-6 mm yr^{-1} for internal deformation of the Caribbean plate, although rigorous estimates await more precise and additional velocities from sites in the plate interior.

Introduction

Prior to GPS-based geodesy, present-day Caribbean plate velocities were estimated using fault azimuths and earthquake slip directions from the complexly deforming Caribbean plate boundaries and indirect constraints imposed by closure of the global plate circuit. Published estimates differ significantly, presumably due to differing prejudices about which data reliably record Caribbean plate motion. For example, estimates of Caribbean-North America (CA-NA) rates range from 11-20 mm yr^{-1} [*Rosencrantz and Mann*, 1991; *DeMets et al.*, 1994] and estimates of CA-NA directions east of Cuba (Fig. 1) range from strike-slip [*Jordan*, 1975; *Minster and Jordan*, 1978; *Stein et al.*, 1988; *DeMets et al.*, 1990, 1994; *Calais and Mercier de Lépinay*, 1993] to ENE-directed convergence [*Deng and Sykes*, 1995]. Deformation of the plate interior has also been proposed [*Heubeck and Mann*, 1991; *Leroy and Mauffret*, 1996].

For these reasons, the Caribbean region was an early target of GPS geodesy and by the mid-1990s, enough GPS velocities existed from the plate interior to construct the first GPS-based kinematic model [*Dixon et al.*, 1998]. Here, we use new geodetic and other data to solve for Caribbean plate angular velocities and to test published models for CA-NA motion. The data include a new GPS velocity from an island (Aves) in the interior of the eastern Caribbean plate (Fig. 1), velocities from significantly extended GPS time series on St. Croix (CRO1), Hispaniola (ROJO), and San Andres island (SANA), and velocities for sixteen GPS stations in the North American plate interior [*DeMets and Dixon*, 1999]. To supplement the still-sparse GPS velocities, we use the azimuths of well-imaged bathymetric lineaments that define the active trace of the eastern Swan Islands transform fault [*Rosencrantz and Mann*, 1991]. These lineaments are morphologically similar to structures that define other active strike-slip faults and thus usefully constrain the CA-NA direction (Table 1).

GPS data analysis and station velocities

Only four GPS sites are located in the Caribbean plate interior (Fig. 1) and have time series long enough to provide a useful velocity (Table 1). Three of these (AVES, ROJO, SANA) have been occupied periodically over intervals ranging from 3.9-7.4 years and CRO1 has operated continuously since late 1995. We omit data collected at ROJO in 1986 [*Dixon et al.*, 1998] because they predate precise orbits and robust terrestrial reference frames. We analyze all GPS data using GIPSY [*Zumberge et al.*, 1997], precise satellite orbits and clocks from JPL and the University of Miami, and following procedures described by *Dixon et al.* [1997]. Free-network station coordinates transformed to ITRF96 [*Sil-*

Table 1. Caribbean kinematic data

Site ID	Lat. (°N)	Long. (°E)	ΔT, #† (yrs)	V_n (mm/yr)	V_e (mm/yr)
GPS velocities relative to ITRF96					
AVES	15.67	-63.62	3.87 yrs,2	14.2±2.2	13.2±2.9
ROJO	17.90	-71.67	4.25 yrs,3	6.9±2.6	13.5±3.0
SANA	12.53	-81.73	7.4 yrs,4	7.4±2.5	14.8±2.7
CRO1	17.76	-64.58	4.05 yrs‡	13.3±2.1	9.8±2.0
Swan Islands transform fault azimuths					
17.63°N	82.60°W	N78°E±2.0	*Rosencrantz and Mann* [1991]		
17.50°N	83.30°W	N74°E±2.0	*Rosencrantz and Mann* [1991]		

† ΔT, # represent the time span of the GPS observations that constrain the velocity and the number of station occupations.
‡ Continuous GPS station.
Correlations between the north and east velocity components are negligible.

1 - Dept. of Geology and Geophysics, UW-Madison
2 - Department of Geology, UPR-Mayagüez
3 - RSMAS, University of Miami
4 - Dept. of Geological Sciences, UC-Boulder
5 - Geosciences Azur, CNRS, Sophia Antipolis, France
6 - Institute for Geophysics, UT-Austin

Paper number 1999GL005436.
0094-8276/00/1999GL005436$05.00

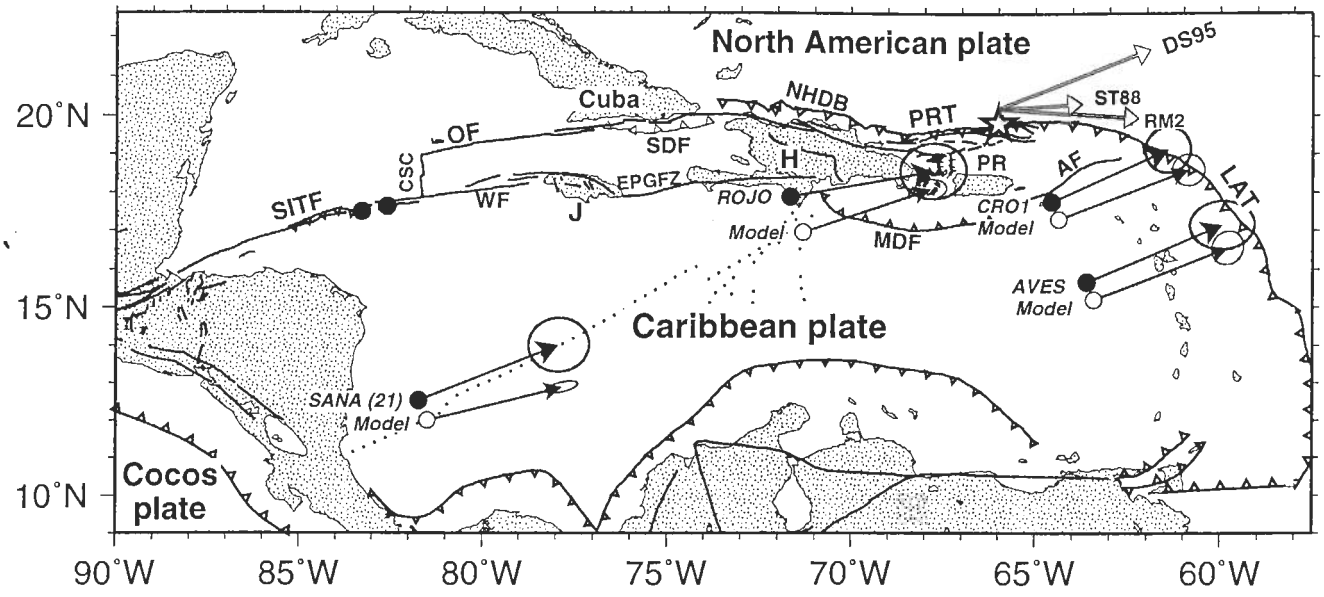

Figure 1. Regional map, locations of data in Table 1 (filled circles), and CA-NA GPS velocities. Ellipses show 2D, 1σ uncertainties. Model velocities (open circles) are computed at GPS station locations using the hybrid CA-NA angular velocity (Table 2). For reference, the velocity at SANA is 21 mm yr^{-1}. Open arrows show CA-NA velocities predicted for a hypothetical site (star) along the Puerto Rico trench by models from *Minster and Jordan* [1978] (RM2), *Stein et al.* [1988] (ST88), and *Deng and Sykes* [1995] (DS95). Abbreviations: H - Hispaniola; J - Jamaica; LAT - Lesser Antilles trench; OF - Oriente fault; PRT - Puerto Rico trench; SDF - Santiago deformed belt; SITF - Swan Islands transform fault.

lard et al., 1998] yield day-to-day repeatabilities in the station latitudes and longitudes of 3-7 millimeters and 6-13 millimeters. Velocity uncertainties are estimated using a model for white- and time-correlated noise in GPS coordinate time series [*Mao et al.*, 1999].

Two of the four GPS sites, ROJO and CRO1, are close enough to plate boundary faults to be affected by elastic strain accumulating along those faults. We thus estimated the potential slip deficit at each site using realistic geometries and maximum slip rates for the nearby fault(s). ROJO lies 55 km south of the Enriquillo fault, with a maximum slip rate of 8 mm yr^{-1} [*Dixon et al.*, 1998], and CRO1 lies 225-250 km south of the Puerto Rico trench and tens of kms from the Anegada passage fault, with respective maximum rates of 18 mm yr^{-1} and ~3 mm yr^{-1} [*Jansma et al.*, 1999]. Forward models of the elastically-induced slip deficit at each site give an upper bound for each of only 1 mm yr^{-1}. To first order, both sites thus move with the stable plate interior.

Table 2. Best-fitting angular velocities

Plate	Data Type	λ (°N)	φ (°E)	ω (°/Myr)	σ_1	σ_2	η (CW)	σ_ω (°/Myr)
CA-IT	GPS†	36.6	275.9	0.295	11.7°	3.0°	-53°	0.074
NA-IT*	GPS	-0.9	280.2	0.192	4.1°	1.6°	-2°	0.009
CA-NA	GPS	69.1	223.3	0.192	31.3°	4.8°	-74°	0.036
CA-IT	Hybrid‡	34.6	269.6	0.334	5.0°	1.3°	-25°	0.043
NA-IT	Hybrid	-1.1	280.4	0.192	4.1°	1.5°	-2°	0.009
CA-NA	Hybrid	64.9	250.5	0.214	14.6°	1.5°	-35°	0.030

† - Only GPS velocities from Table 1 are used.
‡ - All data from Table 1 are used.
* - Angular velocity from *DeMets and Dixon* [1999].

Angular velocities designate motion of the first plate relative to the second. λ, φ, and ω are the latitude, longitude, and angular rotation rate of the best-fitting angular velocity, respectively. σ_1 and σ_2 are lengths of the 2D, 1-sigma semi-major and semi-minor axes of the pole error ellipse. η is the azimuth of σ_1 in degrees CW from north. σ_ω is the 1D standard error for the angular rotation rate. Abbreviations: CA - Caribbean plate; IT - ITRF96; NA - North American plate.

We solve for angular velocities and their uncertainties (Table 2) by minimizing the weighted, least-squares misfit of one or more angular velocities to GPS velocities and geologic data (Table 1) and further requiring that the angular velocities satisfy plate circuit closure [*DeMets et al.*, 1990; *Ward*, 1990]. An angular velocity that best-fits only the four Caribbean GPS velocities (CA-IT in Table 2) yields residual velocities of 0.3-3.2 mm yr^{-1}, averaging 2.0 mm yr^{-1}. The data are thus well fit at the approximate level of their 1.5-3.0 mm yr^{-1} uncertainties. Vector subtraction of a newly published NA-IT angular velocity (Table 2) [*DeMets and Dixon*, 1999] from the CA-IT angular velocity yields a CA-NA angular velocity based solely on GPS observations (Table 1).

To incorporate the additional CA-NA kinematic constraint imposed by the Swan Islands transform fault, we simultaneously inverted data from Table 1 and the 16 North American plate GPS velocities. The fits of the GPS-only and hybrid models to the data are statistically indistinguishable, with differences in their predicted velocities of only 0.2 mm yr^{-1} and 0-6° (Fig. 2). Due to its significantly smaller uncertainties, we hereafter use the hybrid CA-NA angular velocity.

Tests of prior models and model implications

The 19-20 mm yr^{-1} rates predicted by the newly-derived CA-NA angular velocity (Figs. 1 and 2)

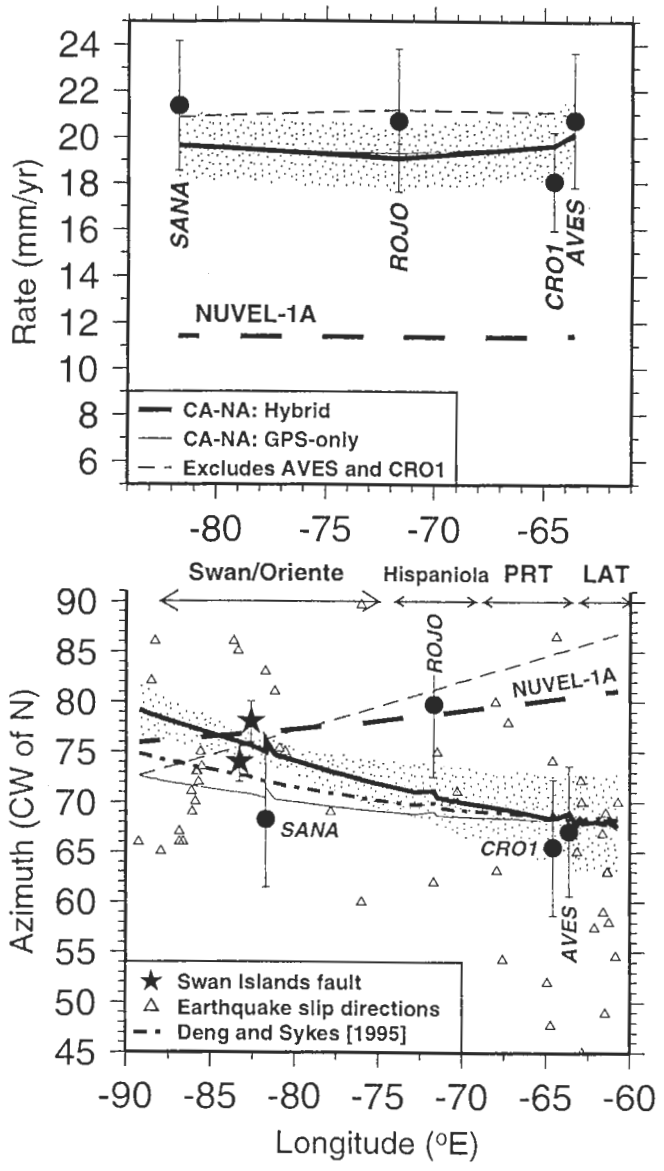

Figure 2. Observed and predicted CA-NA rates and azimuths. Horizontal slip directions (triangles) are for earthquakes from 1957 through March, 1999 and are taken from Harvard centroid moment tensor solutions and *Deng and Sykes* [1995]. Stippled regions show the 1σ prediction uncertainties of the hybrid CA-NA angular velocity. Error bars are one standard error. Abbreviations are from Figure 1.

significantly exceed the 11 mm yr^{-1} rate predicted by the NUVEL-1A model [*DeMets et al.*, 1994], but agree with geodetic rates reported by *Dixon et al.* [1998] and *MacMillan and Ma* [1999] and 10 Myr-average CA-NA rates estimated from magnetic anomalies flanking the Cayman spreading center [e.g. *Rosencrantz*, 1995]. To test whether the CA-NA directions predicted by poles from *Jordan* [1975], *Stein et al.* [1988], *DeMets et al.* [1990], *Calais and Mercier de Lépinay* [1993], and *Deng and Sykes* [1995] differ significantly from those predicted by our hybrid pole, we derived their RMS misfits χ^2 to the data from Table 1 and the 16 NA plate GPS velocities. To do so, we iteratively adjusted the angular rotation rate for each pole until we minimized its RMS misfit; this procedure optimized the fits of previous models to the GPS rates, but not the directions. Respective values of χ^2 for our hybrid model and the above models are 6.5, 33.2, 28.9, 15.1, 45.6, and 12.0.

Comparing the above RMS misfits using an F-test for 2 versus 10-3 degrees of freedom, only the pole from *Deng and Sykes* [1995] fits the data with an RMS misfit not significantly worse than that of the hybrid model. Like the hybrid pole, this pole predicts ENE-directed oblique convergence along the plate boundary east of Cuba. In contrast, the fits of all poles that predict strike-slip motion along the plate boundary east of Cuba are significantly worse than that of the hybrid pole.

Our new model makes useful predictions about boundary-parallel and boundary-normal slip along the CA-NA plate boundary (Fig. 3). For example, the ~45° bend in the northern Lesser Antilles trench requires a ~40% northward decrease in trench-normal convergence rates and a corresponding increase in the trench-parallel slip component (Fig. 3). It is unclear whether the increasingly oblique slip is accommodated via oblique subduction or whether it is instead partitioned and thus accommodated partly by deformation of the Lesser Antilles forearc. The horizontal slip directions for eight out of ten small shallow-thrust earthquakes along the Lesser Antilles trench east of 62°W (Fig. 2) point between the predicted convergence direction and the ~N45°E arc-normal direction, weakly suggesting that partitioning occurs.

Along the northern Hispaniola fold and thrust belt [*Dolan et al.*, 1998], our model predicts boundary-parallel slip of 15±2 mm yr^{-1} (2σ) and boundary-normal convergence of 11±3 mm yr^{-1}. Stream terraces offset by the Septentrional fault of northern Hispaniola yield maximum Holocene strike-slip rates of 13±4 mm yr^{-1} and 23±7 mm

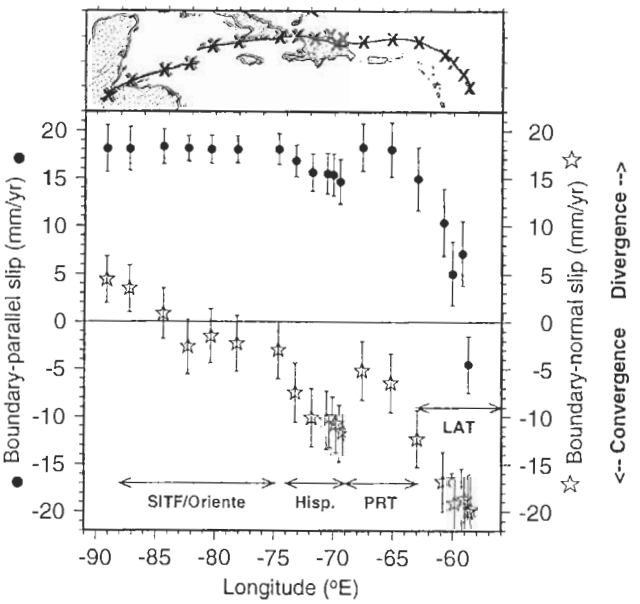

Figure 3. CA-NA velocity components parallel (circles) and perpendicular (stars) to the plate boundary, derived by rotating predicted velocities onto local fault trends at the locations shown by crosses in the upper panel. Uncertainties are 95% and are propagated from the angular velocity covariances. Abbreviations are from Fig. 1.

yr^{-1} [*Mann et al.*, 1998]. These agree well with our estimate of boundary-parallel slip and thus suggest that most boundary-parallel slip is focused along this fault. Farther west, folding and faulting in the Santiago deformed belt south of eastern Cuba [*Calais and Mercier de Lépinay*, 1991] and minor southward thrusting during the May 25, 1992 M_s=6.9 left-lateral strike-slip earthquake southwest of Cuba [*Perrot et al.*, 1997] both support the existence of boundary-normal convergence west of Hispaniola (75°W), where our model predicts 18±2 mm yr^{-1} of boundary-parallel slip and 3±3 mm yr^{-1} of boundary-normal convergence (Fig. 3).

Future tests for plate rigidity

Although the data are presently too sparse and too imprecise to solve for bounds on intra-Caribbean plate deformation, the 2 mm yr^{-1} average misfit of our model to the GPS velocities suggests a crude upper bound of 4-6 mm yr^{-1}. It is certainly premature to rule out slip of several mm yr^{-1} along faults within the plate. For example, the poorly fit direction at ROJO (Fig. 2) may have a tectonic cause given that GPS sites farther north in Hispaniola also move in the same direction (unpublished results). New observations in southern Jamaica and the eastern Honduras, a renewed time series at AVES, which was destroyed by Hurricane Mitch in late 1998, and continued observations at present sites are essential to test whether the Caribbean plate deforms as it is squeezed between the flanking North and South American plates.

Acknowledgements. These measurements were supported by funding from the National Science Foundation and NASA. We thank Cartografia Nacional de Venezuela for arranging permission to occupy the Venezualan island of Aves.

References

Calais, E., and B. Mercier de Lépinay, From transpression to transtension along the northern Caribbean plate boundary: Implications for the recent motion of the Caribbean plate, *Tectonophysics, 186,* 329–350, 1991.

Calais, E., and B. Mercier de Lépinay, Semiquantitative modeling of strain and kinematics along the Caribbean-North America strike-slip plate boundary zone, *J. Geophys. Res., 98,* 8293–8308, 1993.

DeMets, C., and T. Dixon, New kinematic models for Pacific-North America motion from 3 Ma to present, 1: Evidence for steady motion and biases in the NUVEL-1A model, *Geophys. Res. Lett., 26,* 1921–1924, 1999.

DeMets, C., R. G. Gordon, D. F. Argus, and S. Stein, Current plate motions, *Geophys. J. Int., 101,* 425–478, 1990.

DeMets, C., R. G. Gordon, D. F. Argus, and S. Stein, Effect of recent revisions to the geomagnetic reversal timescale on estimates of current plate motions, *Geophys. Res. Lett., 21,* 2191–2194, 1994.

Deng, J., and L. R. Sykes, Determination of Euler pole for contemporary relative motion of Caribbean and North American plates using slip vectors of interplate earthquakes, *Tectonics, 14,* 39–53, 1995.

Dixon, T. H., A. Mao, M. Bursik, M. Heflin, J. Langbein, R. Stein, and F. Webb, Continuous monitoring of surface deformation at Long Valley Caldera, California, with GPS, *J. Geophys. Res., 102,* 12,017–12,034, 1997.

Dixon, T. H., F. Farina, C. DeMets, P. Jansma, P. Mann, and E. Calais, Relative motion between the Caribbean and North American plates and related boundary zone deformation from a decade of GPS observations, *J. Geophys. Res., 103,* 15,157–15182, 1998.

Dolan, J. F., H. Mullins, H. T. Mullins, and D. J. Wald, Active tectonics of the north-central Caribbean: Oblique collision, strain partitioning, and opposing subducted slabs, in *Active strike-slip and collisional tectonics of the northern Caribbean Plate boundary zone, GSA Special Paper 326,* edited by J. F. Dolan and P. Mann, pp. 1–61, GSA, Boulder, 1998.

Heubeck, C., and P. Mann, Geologic evaluation of plate kinematic models for the North American-Caribbean plate boundary zone, *Tectonophysics, 191,* 1–26, 1991.

Jansma, P. E., A. Lopez, G. S. Mattioli, C. DeMets, T. H. Dixon, P. Mann, E. Calais, Neotectonics of Puerto Rico and the Virgin Islands, northeastern Caribbean, from GPS geodesy, *Tectonics*, submitted, 9/1999.

Jordan, T. H., The present-day motions of the Caribbean plate, *J. Geophys. Res., 80,* 4433–4439, 1975.

Leroy, S., and A. Mauffret, Intraplate deformation in the Caribbean region, *J. Geodynamics, 21,* 113–122, 1996.

MacMillan, D. S., and C. Ma, VLBI measurements of Caribbean and South American motion, *Geophys. Res. Lett., 26,* 919–922, 1999.

Mann, P., C. S. Prentice, G. Burr, and F. W. Taylor, Tectonic geomorphology and paleoseismicity of the Septentrional fault system, Dominicann Republic, *Geol. Soc. Amer. Special Paper 326,* 63-124, 1998.

Mao, A., C. G. A. Harrison, and T. H. Dixon, Noise in GPS coordinate time series, *J. Geophys. Res., 104,* 2797–2816, 1999.

Minster, J. B., and T. H. Jordan, Present-day plate motions, *J. Geophys. Res., 83,* 5331–5354, 1978.

Perrot, J., E. Calais, and B. Mercier de Lepinay, Waveform simulation of the May 25th, 1992, M_S=6.7 Cabo Cruz earthquake (Cuba): New constraints on the tectonic regime along the northern Caribbean plate boundary, *Pure and Applied Geophys., 149,* 475–487, 1997.

Rosencrantz, E., and P. Mann, SeaMARC II mapping of transform faults in the Cayman Trough, Caribbean Sea, *G, 19,* 690–693, 1991.

Sillard, P., Z. Altamimi, and C. Boucher, The ITRF96 realization and its associated velocity field, *Geophys. Res. Lett., 25,* 3222–3225, 1998.

Stein, S., C. DeMets, R. G. Gordon, J. Brodholt, J. F. Engeln, D. A. Wiens, D. Argus, P. Lundgren, C. Stein, and D. Woods, A test of alternative Caribbean plate relative motion models, *J. Geophys. Res., 93,* 3041–3050, 1988.

Ward, S. N., Pacific-North America plate motions: New results from very long baseline interferometry, *J. Geophys. Res., 95,* 21,965–21,981, 1990.

Zumberge, J. F., M. B. Heflin, D. C. Jefferson, M. M. Watkins, and F. H. Webb, Precise point positioning for the efficient and robust analysis of GPS data from large networks, *J. Geophys. Res., 102,* 5005–5017, 1997.

C. DeMets, Geology and Geophysics, UW-Madison, 1215 W Dayton St., Madison, WI 53706. (chuck@geology.wisc.edu)

P. Jansma and G. Mattioli, Dept. of Geology, UPR-Mayagüez, Mayaguez, PR 00681-9017

T. Dixon and F. Farina, RSMAS, University of Miami, 4600 Rickenbacker Causeway, Miami, FL 33149-1098

R. Bilham, CIRES/449, Boulder, CO 80309-0216

E. Calais, CNRS-Geosciences Azur, 250 Rue Albert Einstein, Valbonne 06560, France

P. Mann, Institute for Geophysics, UT-Austin, Austin, TX 78759-8500

(Received: September 16, 1999; Revised: December 06, 1999; Accepted December 22, 1999)